Coordination Polymers

International Edition: DOI: 10.1002/anie.201600123
German Edition: DOI: 10.1002/ange.201600123

Glass Formation of a Coordination Polymer Crystal for Enhanced Proton Conductivity and Material Flexibility

Wenqian Chen, Satoshi Horike, Daiki Umeyama, Naoki Ogiwara, Tomoya Itakura, Cédric Tassel, Yoshihiro Goto, Hiroshi Kageyama, and Susumu Kitagawa**

Abstract: *The glassy state of a two-dimensional (2D) Cd^{2+} coordination polymer crystal was prepared by a solvent-free mechanical milling process. The glassy state retains the 2D structure of the crystalline material, albeit with significant distortion, as characterized by synchrotron X-ray analyses and solid-state multinuclear NMR spectroscopy. It transforms to its original crystal structure upon heating. Thus, reversible crystal-to-glass transformation is possible using our new processes. The glass state displays superior properties compared to the crystalline state; specifically, it shows anhydrous proton conductivity and a dielectric constant two orders of magnitude greater than the crystalline material. It also shows material flexibility and transparency.*

Coordination polymer (CP) crystals are an attractive class of solid materials, which demonstrate porosity, and catalytic, magnetic, dielectric, and conductive behavior.[1] CP crystals are constructed from metal ions and bridging ligands by self-assembly, and the wide array of observed crystal structures have contributed to their attractive functionalities. In recent times, a number of reports investigating the control of disorder in CP structures have appeared. In the field of porous CPs (PCPs) and metal–organic frameworks (MOFs), which are categorized as CPs having potential voids,[2] there have been many studies on defect engineering,[3] solid solution formation,[4] and amorphous states.[5] The design of disorder in CP crystals involving PCPs and MOFs, with a view to expanding and improving the functionalities of the materials, is an emerging area of research.

[*] Dr. W. Chen, Dr. S. Horike, Dr. D. Umeyama, N. Ogiwara, Prof. S. Kitagawa
Department of Synthetic Chemistry and Biological Chemistry
Graduate School of Engineering, Kyoto University
Katsura, Nishikyo-ku, Kyoto 615–8510 (Japan)
E-mail: horike@sbchem.kyoto-u.ac.jp
kitagawa@icems.kyoto-u.ac.jp
T. Itakura
DENSO CORPORATION
1-1 Showa-cho, Kariya, Aichi 448–8661 (Japan)
Dr. C. Tassel, Y. Goto, Prof. H. Kageyama
Department of Energy and Hydrocarbon Chemistry
Graduate School of Engineering, Kyoto University
Katsura, Nishikyo-ku, Kyoto 615–8510 (Japan)
Prof. S. Kitagawa
Institute for Integrated Cell-Material Sciences (WPI-iCeMS)
Kyoto University, Yoshida, Sakyo-ku, Kyoto 606–8501 (Japan)

Supporting information for this article can be found under: http://dx.doi.org/10.1002/anie.201600123.

The glassy state is regarded as a very disordered state, and is defined as an amorphous solid showing glass transition behavior.[6] Preparation of a glassy state from a crystalline solid is one of the main subjects in materials chemistry, because the unique properties; transparency, network dynamics, and mechanical flexibility of glassy states are not possible in the crystalline state. The properties permit the preparation of various optical devices, ion/electron conductors, and high strength/toughness materials. The most popular approach to prepare the glass from crystals is melt-quenching. However, application of this technique to CP crystals is difficult, because most of them do not have a stable liquid state. There are a few exceptions: Bennett, Greaves, and co-workers fabricated the glassy state of $[Zn(imidazolate)_2]$ (ZIF-4) crystals by crystal melting at 327 °C.[7] Our group found several CP crystals showing melting behavior below 200 °C, and their glassy states were processable.[8] However, the chemistry and material properties of the glassy state of the CP crystals is not well understood because the melting behavior is rarely observed. To shed light on the potential of the glassy state of CP crystals, in this work, we demonstrate the preparation of glass from a non-melting CP crystal by solvent-free ball milling. We characterized its glass-formation behavior and the structure of the glassy state. As a result, unique functions and properties of the glassy state, such as enhanced proton conductivity, increased dielectric constant, and material flexibility and transparency, were discovered. These are not present in its crystalline state.

We synthesized two-dimensional (2D) CP crystals of the formula $[Cd(H_2PO_4)_2(1,2,4\text{-triazole})_2]$ (CdTz). The X-ray crystal structure of CdTz is shown in Figure 1 a. The crystals are composed of octahedrally coordinated Cd^{2+} ions with mono-coordinated dihydrogen phosphate ($H_2PO_4^-$) and bridging 1,2,4-triazole ligands, which form extended 2D layers. The layers stack mutually, and $H_2PO_4^-$ coordinates to Cd^{2+} in the axial positions. The structure is nonporous and an isostructure of $[Zn(H_2PO_4)_2(1,2,4\text{-triazole})_2]$ (ZnTz).[9] CdTz can also be described as a "dense MOF", since the 1,2,4-triazole rings bridge two Cd^{2+} ions to form a 2D structure.[10] We conducted the ball milling treatments for CdTz under an Ar atmosphere. Milling times were 40, 240, and 500 minutes and we denote these products as *a*-CdTz-*x* (where *x* = milling time). The powder X-ray diffraction (PXRD) patterns of powder samples of CdTz and *a*-CdTz-*x* are shown in Figure 1 b. The CdTz pattern is identical to the simulated pattern calculated from the single-crystal structure. The patterns of *a*-CdTz-*x* show broad diffuse scattering, indicating that the samples are amorphous in nature. Amorphization is widely observed when PCP/MOFs are

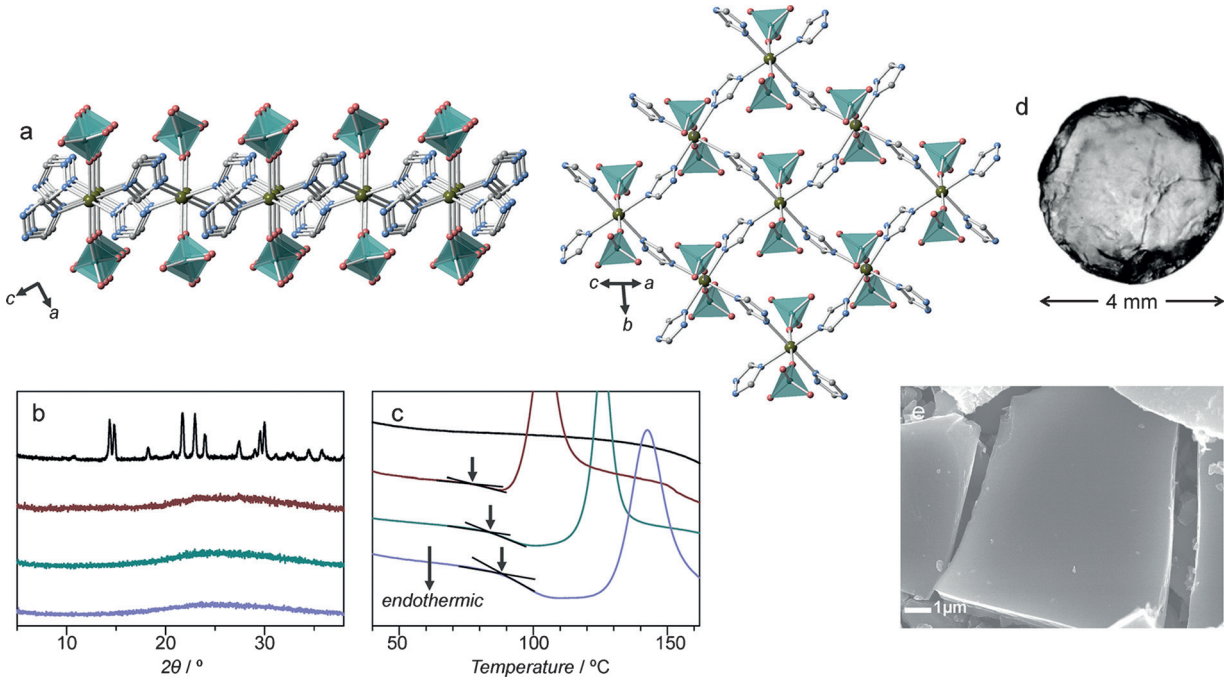

Figure 1. a) Crystal structure of CdTz at 20 °C. Gray, sky blue, pink, yellow green, deep green are C, N, O, Cd, P. b) Powder X-ray diffraction, and c) DSC in the first heating process of CdTz (black), *a*-CdTz-40 (brown), *a*-CdTz-240 (green), *a*-CdTz-500 (purple). Glass transition temperature (T_g) are shown as an arrow. The heating rate was 10 °C min^{-1}. d) Photo and e) SEM image of a *a*-CdTz-240 pellet prepared at a pressure of 4 GPa.

treated by mechanical milling or under high pressure.[5b,c,11] The thermogravimetric analysis with mass spectroscopy (TGA-MS) profile of CdTz (see Figure S1 in the Supporting Information) shows no clear weight loss below 160 °C and a gradual decrease above 160 °C. This decrease is due to the elimination of 1,2,4-triazole and the condensation of H_2PO_4 groups. The TGA profiles of *a*-CdTz-*x* show a gradual release of physically bound H_2O between 25 and 150 °C (because these samples are hydrophilic and treated under air), and the decomposition temperatures are same as CdTz (160 °C). This suggests the formulas of CdTz and the three *a*-CdTz-*x* samples are the same and remain intact until 160 °C.

We characterized the thermal behavior of CdTz and *a*-CdTz-*x* by the use of differential scanning calorimetry (DSC, 10 °C min^{-1}, Figure 1 c) in Ar atmosphere. In the first heating process, CdTz does not show any peak indicating that its crystalline state is intact, and it does not have a melting point. Meanwhile, each *a*-CdTz-*x* sample exhibits a typical profile for glass, and contains endothermic glass transitions (T_g) and exothermic crystallizations (T_c). The T_g and T_c values for *a*-CdTz-*x* are 79/104 °C (*a*-CdTz-40), 85/126 °C (*a*-CdTz-240), and 90/142 °C (*a*-CdTz-500), respectively. The presence of T_g and T_c and their dependence on ball milling condition suggests that all *a*-CdTz-*x* samples are in a glassy state below T_g. Most of the amorphous PCP/MOFs prepared by milling procedures do not show this crystallization, but decompose upon heating. Meanwhile, when ball milling is used to prepare glass for other materials; various organic crystals and inorganic crystals often yield vitreous states.[6c,12] We measured the temperature-dependent structure function for *a*-CdTz-240, and the amorphous pattern at 25 °C changed to a crystalline state corresponding to CdTz above T_c (Figure S2). The mechanical energy imparted by milling processes can be stored in solids,[13] and a longer ball milling time introduces higher energy to the crystalline state and permits formation of the glassy state. For many solids, the enthalpy of crystallization depends on the ball milling conditions. The enthalpies of crystallization for *a*-CdTz-*x* are -37 ± 1 J g^{-1} (*a*-CdTz-40), -46 ± 1 J g^{-1} (*a*-CdTz-240), and -48 ± 1 J g^{-1} (*a*-CdTz-500). These are comparable to those of several organic polymers, such as poly(lactic acid), and inorganic solids, including the metallic glass $Pd_{39}Ni_{10}Cu_{30}P_{21}$.[14] To demonstrate the glass characteristics, we fabricated a millimeter-sized transparent glass pellet of *a*-CdTz-240 (Figure 1 d). A pellet of *a*-CdTz-240 powder with a diameter of 4.2 mm and 1.0 mm of height was prepared, and pressed under 4 GPa at 70 °C for 2 hours. The pressure treatment formed transparent glass. The SEM image of the particle surface of this sample, shown in Figure 1 e, displays a smooth and crack-free texture. The pressure-based transformation did not yield a transparent pellet when we used CdTz as the substrate material. The mechanical properties of *a*-CdTz-*x* offer a significant advantage as a material, because the glass pellet does not have a grain boundary and it is useful as an ion conductive material, which will be discussed in further detail below.

Understanding the structure of *a*-CdTz-*x* and whether it is related to the crystalline state CdTz is important. For example, the glassy state of ZIF-4, prepared by melt-quenching, has a 3D networked structure with tetrahedral Zn^{2+}-N clusters.[7] The glassy state of ZnTz, also prepared by melt-quenching, is composed of discrete Zn^{2+} complexes and is not a networked structure.[8b] These studies suggest that the glassy states of CP crystals depend on various structural parameters.

We measured the X-ray absorption spectrum (XAS) for CdTz to understand the local structural arrangement around Cd^{2+} centers. The X-ray absorption near-edge structure (XANES) spectra of CdTz and *a*-CdTz-240 shown in Figure 2a (inset) are identical, and the coordination geometry of Cd^{2+} (Figure S3) at the nearest neighbors remains octahedral after the vitrification. Fourier-transformed Cd K-edge EXAFS spectra of CdTz and *a*-CdTz-240 with peak assignments are shown in Figure 2a. In the spectra, some peaks corresponding to *a*-CdTz-240 are less intense than those of CdTz, especially at 1.7 and 3.3 Å, which is due to ligand disorder in the glassy state. Thus we consider that the Cd^{2+} ions in *a*-CdTz-240 are coordinated by $H_2PO_4^-$ and 1,2,4-triazole in a distorted octahedral arrangement.

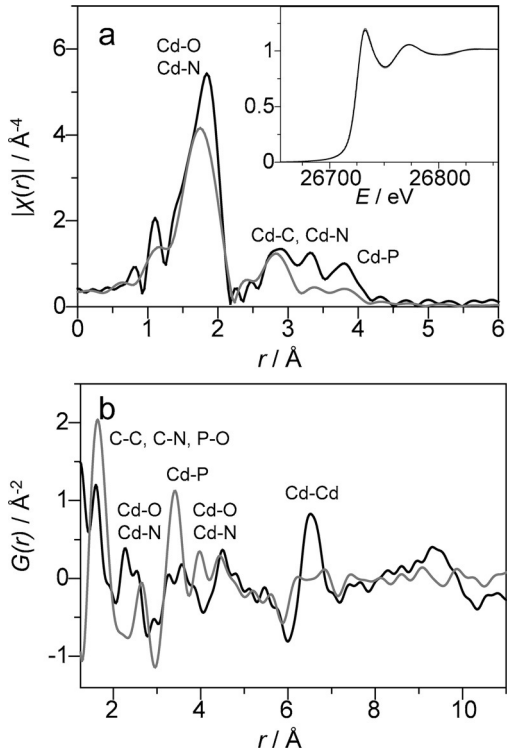

Figure 2. a) FT-EXAFS and XANES (inset) spectra of *a*-CdTz-240 (light gray) and CdTz (black) at 25 °C. b) PDF of *a*-CdTz-240 (light gray), and the comparison of the short-range PDFs of CdTz (black) and *a*-CdTz-240 (light gray) at 25 °C.

To better understand the structure of the glassy state, X-ray total scattering structure functions, $S(Q)$, and the corresponding reduced pair distribution functions, $G(r)$, of CdTz and *a*-CdTz-240 were collected in Ar atmosphere (Figure 2b). The peak at 1.5 Å for both samples is due to the nearest neighbor of C–C, C–N, and P–O in the 1,2,4-triazole and $H_2PO_4^-$ ligands. The $G(r)$ of CdTz show sharp peaks up to r of 30 Å (Figure S4), and the intense peak at 6.5 Å corresponds to Cd^{2+}-Cd^{2+} periodicity. In contrast, the $G(r)$ of *a*-CdTz-240 shows a broad feature at 6.5 Å. This indicates that *a*-CdTz-240 does not have a periodic order of Cd^{2+}-Cd^{2+}, and it supports the distorted structure model of *a*-CdTz-240. We also found a substantial change at r of 2.2 Å, attributed to Cd–O and Cd–N, following the vitrification, but it is difficult to discuss the change of coordination geometry around Cd^{2+} ions.[15] We performed variable temperature MAS solid-state ^{13}C NMR spectroscopy for *a*-CdTz-240 (Figure 3a). The two broad peaks at 144 and 149 ppm at 23 °C are due to the disordered 1,2,4-triazole rings.[16] At 80 °C, the two peaks of 1,2,4-triazole become sharper and shift to 148 and 150 ppm because of the crystallization that occurs at this temperature. T_c at 80 °C observed by NMR spectroscopy is lower than that from DSC. T_c is influenced by the heating program (ramping rate, temperature holding time) and other physical stimulus. The solid-state NMR measurement requires long time and a MAS process for each spectrum collection. These factors promoted the crystallization at lower temperature compared with the DSC results.

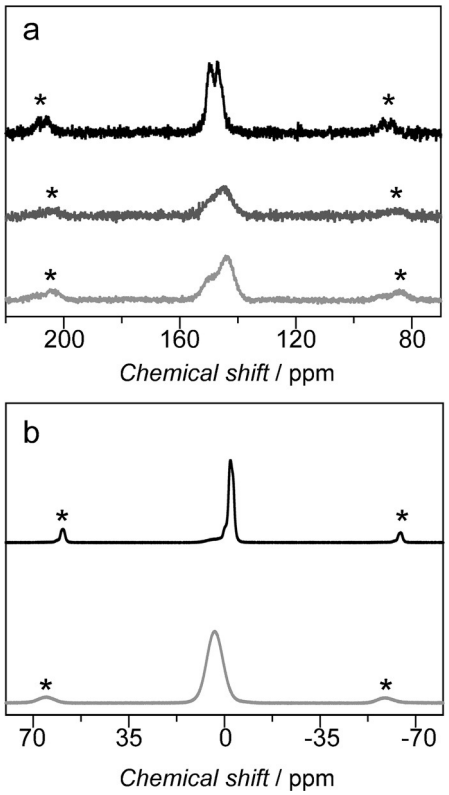

Figure 3. a) Variable temperature MAS solid state ^{13}C NMR spectra of *a*-CdTz-240 at 23 °C (light gray), 58 °C (dark gray), 80 °C (black). b) Solid state ^{31}P NMR spectra of CdTz (black) and *a*-CdTz-240 (light gray) at 23 °C. The frequency of magic angle spinning for ^{13}C NMR was 6 kHz and for ^{31}P NMR was 10 kHz. Asterisks denote spinning side bands.

The ^{113}Cd NMR spectra of both CdTz and *a*-CdTz-40 (Figure S5) have a single peak at 150 ppm, and the chemical shift is in the range consistent with an octahedral coordination geometry around Cd^{2+}.[17] These data support the results of the XAS studies. The low signal-to-noise ratio for the peaks of *a*-CdTz-40 is suggestive of the distorted coordination geometry around Cd^{2+}, which supports the PDF results. The ^{31}P NMR spectrum of CdTz (Figure 3b) displays a sharp isotropic peak at −3 ppm, which is due to mono-coordinating

$H_2PO_4^-$. *a*-CdTz-240 has broad peaks, and the main peak appears at 3 ppm. The chemical shift of the peaks is in the range of mono-coordinating dihydrogen phosphate ligands.[18] Based on these analyses, we conclude that *a*-CdTz-*x* preserves the 2D layered network structure that originated from CdTz, and that the long-range order in the structure is lost because of the distortion around the Cd^{2+} center.

Unique optical or conductive functions are often expected in glassy state CPs.[19] In the field of solid-state ionics, the fabrication of materials in a glassy state has been one of the main approaches for developing materials that display higher ion conductivities than their crystalline state.[20] Glassy states usually have open network structures and display high mobility of the ion carrier; these characteristics are suitable for fast ion conduction. Crystalline CdTz has acidic $H_2PO_4^-$ groups that form extended hydrogen-bonded networks, which would function as a proton hopping path. Figure 4a (black) shows the proton conductivity of CdTz in an Ar atmosphere, measured by AC impedance spectroscopy. The compound shows low conductivity: 4×10^{-10} S cm^{-1} at 50 °C and 8×10^{-7} S cm^{-1} at 150 °C. The activation energy for the conductivity is 1.0 eV, which is comparable to that of some acceptor-doped $BaZrO_3$.[21] The low proton conductivity is because $H_2PO_4^-$ groups mutually interact through hydrogen bonds, and each proton is hard to be dynamic for fast conduction. As shown in Figure 4a, the proton conductivities of *a*-CdTz-*x* below their T_c are over two orders of magnitude higher than those of CdTz: *a*-CdTz-40, *a*-CdTz-240, and *a*-CdTz-500 show proton conductivities of 1.0×10^{-6}, 5.4×10^{-5}, and 1.0×10^{-4} S cm^{-1}, respectively, at just below each T_c. Note the T_cs in this case are determined with a heating rate of 1.3 °C min^{-1}, and are lower than those from the DSC shown in Figure 1c (measured at 10 °C min^{-1}). In addition, we observed a conductivity drop above T_c accompanied by crystallization from *a*-CdTz-*x* to CdTz, and conductivities gradually approach the same value as CdTz. On the other hand, we did not observe differences in the conductivity at T_g for all *a*-CdTz-*x*. This suggests that there is little correlation between the structural relaxation mode near T_g and the electric relaxation mode for ionic conductivity. The total proton conductivities are fitted as a function of temperature following the Arrhenius equation, $\sigma = (\sigma_0/T)\exp(-E_a/k_BT)$, where E_a is the activation energy for ionic conduction, and k_B is the Boltzmann constant. σ_0 is a pre-exponential factor, and it is mainly explained by the concentration of mobile ions.[22] The activation energies for proton conductivity in the three *a*-CdTz-*x* compounds were 1.2 eV in the temperature range between 30 and 90 °C, which is higher than that of CdTz (1.0 eV). Disappearance of long-range order in the structure of *a*-CdTz-*x* would prevent effective proton hopping, resulting in a higher activation energy for conduction. On the other hand, logσ_0, for *a*-CdTz-40 was 14.8, calculated in the temperature range between 34 and 88 °C, which is much greater than for CdTz (8.5). The higher σ_0 observed for the amorphous state compared with the crystalline state is also observed in other inorganic conductors such as fluorophosphate $Na_3Al_2(PO_4)_2F_3$.[23] The downfield chemical shift (6 ppm) in the ^{31}P NMR spectrum of *a*-CdTz-*x* compared with CdTz also suggests that the acidity of $H_2PO_4^-$ in the structure is enhanced by the glass formation, resulting in higher proton conductivity.[24] We also performed impedance spectroscopy measurements on *a*-CdTz-240 under 4 GPa pressure (Figure 4b, open circles). The observed conductivity plot under 4 GPa pressure is different from that under ambient pressure (0.1 MPa). The profile under high pressure linearly increases as temperature increases, without crystallization. At 150 °C, the conductivity was 7.4×10^{-6} S cm^{-1}, while the activation energy was 0.76 eV. These values are lower than those of CdTz and *a*-CdTz-*x* at 0.1 MPa. We assume that the applied high pressure suppresses the molecular motion in *a*-CdTz-240, and prohibits the crystallization to CdTz. The pellet maintained the glassy state after the high pressure impedance measurement was concluded, which was checked by PXRD (Figure S6). We measured the dielectric constants, ε', of CdTz and *a*-CdTz-240 as a function of temperature, using AC impedance spectroscopy. Figure 4c and d show the temperature dependence of ε' for CdTz and *a*-CdTz-240. ε' for CdTz increases upon heating, and it is 73 at 150 °C at a frequency of 100 Hz. The gradual increase upon heating is due to the thermal activation of polar groups in the structure. The

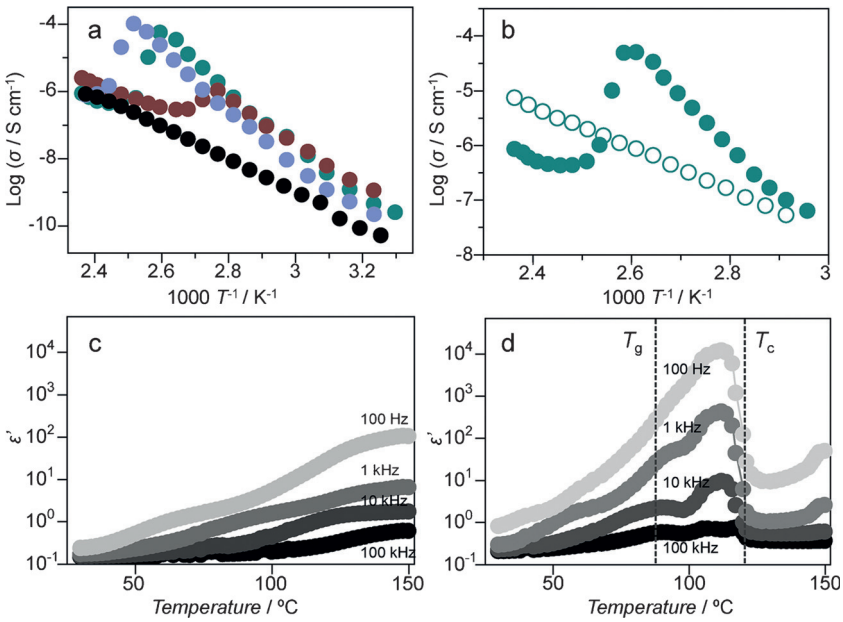

Figure 4. a) Temperature-dependent proton conductivities of CdTz (black), *a*-CdTz-40 (brown), *a*-CdTz-240 (green), and *a*-CdTz-500 (purple) under an Ar atmosphere. The heating rate was 1.3 °C min^{-1}. b) Temperature-dependent proton conductivities of *a*-CdTz-240 under 1 atm (solid green) and 4 GPa (open green). Temperature dependent dielectric constant of c) CdTz and d) *a*-CdTz-240 at frequencies between 100 Hz and 100 KHz. The two dot lines in (d) are T_g and T_c obtained from the DSC results.

profiles of ε' for *a*-CdTz-240 show differences from those of CdTz, and all of the profiles under a number of frequencies between 100 Hz and 100 kHz have local maximum points at 112 °C. ε' reaches 104 at 100 Hz and 600 at 1 kHz. The temperature at which the highest dielectric constants occurred is identical to the temperature of highest conductivity as shown in Figure 4a (green), where it is slightly below T_c. ε' for both CdTz and *a*-CdTz-240 depend heavily on the AC frequency, and it suggests the observed dielectric constant originates from the large polar 1,2,4-triazole or $H_2PO_4^-$ groups in the structure. The distortion in the structure of *a*-CdTz-240 enhances the molecular (and ionic) motions and contributes to the improved proton conductivity and the large ε' compared with crystalline state.

In conclusion, we discovered a non-thermal method for the synthesis of the glassy state of a 2D CP crystals by the use of solvent-free ball milling of a crystalline material. The resulting samples showed clear glass transition and crystallization, and also changed to transparent bulk glass under the applied pressure. Synchrotron X-ray measurements and solid state NMR spectra suggest that the 2D metal-organic coordination networks are preserved in the glassy state. After vitrification, significant enhancements in proton conductivity and dielectric constant were found, due to the disorder and enhanced mobility of ligands in the glassy structure. The ball milling treatment is widely available to convert non-melting CP crystals, including PCPs and MOFs, to a glassy state. This work demonstrates the great potential of the glassy state of CP crystals in terms of their physical functions (conductivity, increased dielectric constant), and optical properties that depend on transparency, and material flexibility.

Experimental Section

Synthesis of powder samples of $[Cd(H_2PO_4)_2(1,2,4\text{-triazole})_2]$ (CdTz) was conducted by solid state mechanical milling process.[25] $Cd(OAc)_2{\cdot}2H_2O$ (266 mg, 1 mmol), 1,2,4-triazole (138 mg, 2 mmol), and phosphoric acid (85 %, 134 μL, 2 mmol) were mixed into a mortar and ground for 30 minutes. The powder obtained was washed with ethanol three times, and dried at 25 °C under vacuum overnight. For the preparation of *a*-CdTz-*x*, we conducted ball milling for CdTz for 40, 240, 500 minutes under Ar in a planetary ball-milling apparatus with zirconia vessel and balls at 400 rpm. The X-ray absorption spectrum (XAS) of the Cd^{2+} of CdTz and *a*-CdTz-*x* were collected under Ar atmosphere at the beamline BL07 at SAGA Light Source. The pair distribution function (PDF) for CdTz and *a*-CdTz-*x* were obtained from X-ray total scattering measurements. The data were collected at 25 °C and under Ar atmosphere using a large Debye–Scherrer camera with an imaging-plate-type detector, installed in the BL02B2 beamline at SPring-8. The incident beam was monochromated at $\lambda = 0.35314$ Å. The pressure dependency of the preparation of transparent glass was performed with a cubic-anvil high pressure apparatus known as the DIA.

Acknowledgements

We acknowledge Dr. Masahide Kawamoto at Kyushu Synchrotron Light Research Center for XAS measurements of Cd, and Dr. Shogo Kawaguchi at Super Photon ring-8 GeV (SPring-8) for PXRD measurements for PDF analyses, and Dr. Maw Lin Foo for helpful discussion. This work was supported by the PRESTO and A-STEP of the Japan Science and Technology Agency (JST), CREST of the JST, a Grant-in-Aid for Scientific Research on the Innovative Areas: "Fusion Materials", Grant-in-Aid for Young Scientists (A), Grant-in-Aid for Challenging Exploratory Research from the Ministry of Education, Culture, Sports, Science and Technology, Japan.

Keywords: coordination polymers · glasses · mechanical properties · mechanochemistry · proton conductivity

How to cite: *Angew. Chem. Int. Ed.* **2016**, *55*, 5195–5200
Angew. Chem. **2016**, *128*, 5281–5286

[1] a) S. R. Batten, R. Robson, *Angew. Chem. Int. Ed.* **1998**, *37*, 1460–1494; *Angew. Chem.* **1998**, *110*, 1558–1595; b) M. Eddaoudi, D. B. Moler, H. Li, B. Chen, T. M. Reineke, M. O'Keeffe, O. M. Yaghi, *Acc. Chem. Res.* **2001**, *34*, 319–330; c) B. Moulton, M. J. Zaworotko, *Chem. Rev.* **2001**, *101*, 1629–1658; d) S. Kitagawa, R. Kitaura, S. Noro, *Angew. Chem. Int. Ed.* **2004**, *43*, 2334–2375; *Angew. Chem.* **2004**, *116*, 2388–2430; e) J. Lee, O. K. Farha, J. Roberts, K. A. Scheidt, S. T. Nguyen, J. T. Hupp, *Chem. Soc. Rev.* **2009**, *38*, 1450–1459; f) D. F. Weng, Z. M. Wang, S. Gao, *Chem. Soc. Rev.* **2011**, *40*, 3157–3181; g) G. Givaja, P. Amo-Ochoa, C. J. Gomez-Garcia, F. Zamora, *Chem. Soc. Rev.* **2012**, *41*, 115–147.

[2] S. R. Batten, N. R. Champness, X.-M. Chen, J. Garcia-Martinez, S. Kitagawa, L. Öhrström, M. O'Keeffe, M. Paik Suh, J. Reedijk, *Pure Appl. Chem.* **2013**, *85*, 1715–1724.

[3] a) Z. Sun, T. Chen, J. Luo, M. Hong, *Angew. Chem. Int. Ed.* **2012**, *51*, 3871–3876; *Angew. Chem.* **2012**, *124*, 3937–3942; b) H. Wu, Y. S. Chua, V. Krungleviciute, M. Tyagi, P. Chen, T. Yildirim, W. Zhou, *J. Am. Chem. Soc.* **2013**, *135*, 10525–10532; c) R. Ameloot, F. Vermoortele, J. Hofkens, F. C. De Schryver, D. E. De Vos, M. B. Roeffaers, *Angew. Chem. Int. Ed.* **2013**, *52*, 401–405; *Angew. Chem.* **2013**, *125*, 419–423; d) M. J. Cliffe, W. Wan, X. Zou, P. A. Chater, A. K. Kleppe, M. G. Tucker, H. Wilhelm, N. P. Funnell, F. X. Coudert, A. L. Goodwin, *Nat. Commun.* **2014**, *5*, 4176; e) J. M. Taylor, S. Dekura, R. Ikeda, H. Kitagawa, *Chem. Mater.* **2015**, *27*, 2286–2289.

[4] a) H. Deng, C. J. Doonan, H. Furukawa, R. B. Ferreira, J. Towne, C. B. Knobler, B. Wang, O. M. Yaghi, *Science* **2010**, *327*, 846–850; b) T. Fukushima, S. Horike, Y. Inubushi, K. Nakagawa, Y. Kubota, M. Takata, S. Kitagawa, *Angew. Chem. Int. Ed.* **2010**, *49*, 4820–4824; *Angew. Chem.* **2010**, *122*, 4930–4934; c) A. D. Burrows, *CrystEngComm* **2011**, *13*, 3623.

[5] a) R. P. Swatloski, S. K. Spear, J. D. Holbrey, R. D. Rogers, *J. Am. Chem. Soc.* **2002**, *124*, 4974–4975; b) K. W. Chapman, G. J. Halder, P. J. Chupas, *J. Am. Chem. Soc.* **2009**, *131*, 17546–17547; c) K. Ohara, J. Marti-Rujas, T. Haneda, M. Kawano, D. Hashizume, F. Izumi, M. Fujita, *J. Am. Chem. Soc.* **2009**, *131*, 3860–3861; d) T. D. Bennett, A. L. Goodwin, M. T. Dove, D. A. Keen, M. G. Tucker, E. R. Barney, A. K. Soper, E. G. Bithell, J. C. Tan, A. K. Cheetham, *Phys. Rev. Lett.* **2010**, *104*, 115503.

[6] a) P. G. Debenedetti, F. H. Stillinger, *Nature* **2001**, *410*, 259–267; b) K. J. Rao, *Structural Chemistry of Glasses*, Elsevier, Amsterdam, **2002**; c) I. Sestak, W. Distler, J. F. Forbes, M. Dowsett, A. Howell, J. Cuzick, *J. Clin. Oncol.* **2010**, *28*, 3411–3415.

[7] T. D. Bennett, J. C. Tan, Y. Yue, E. Baxter, C. Ducati, N. J. Terrill, H. H. Yeung, Z. Zhou, W. Chen, S. Henke, A. K. Cheetham, G. N. Greaves, *Nat. Commun.* **2015**, *6*, 8079.

[8] a) S. Horike, D. Umeyama, M. Inukai, T. Itakura, S. Kitagawa, *J. Am. Chem. Soc.* **2012**, *134*, 7612–7615; b) D. Umeyama, S.

Horike, M. Inukai, T. Itakura, S. Kitagawa, *J. Am. Chem. Soc.* **2015**, *137*, 864 – 870.
[9] D. Umeyama, S. Horike, M. Inukai, T. Itakura, S. Kitagawa, *J. Am. Chem. Soc.* **2012**, *134*, 12780 – 12785.
[10] a) J. C. Rybak, M. Hailmann, P. R. Matthes, A. Zurawski, J. Nitsch, A. Steffen, J. G. Heck, C. Feldmann, S. Gotzendorfer, J. Meinhardt, G. Sextl, H. Kohlmann, S. J. Sedlmaier, W. Schnick, K. Müller-Buschbaum, *J. Am. Chem. Soc.* **2013**, *135*, 6896 – 6902; b) G. Lorusso, J. W. Sharples, E. Palacios, O. Roubeau, E. K. Brechin, R. Sessoli, A. Rossin, F. Tuna, E. J. McInnes, D. Collison, M. Evangelisti, *Adv. Mater.* **2013**, *25*, 4653 – 4656; c) S. Tominaka, F. X. Coudert, T. D. Dao, T. Nagao, A. K. Cheetham, *J. Am. Chem. Soc.* **2015**, *137*, 6428 – 6431.
[11] a) Y. H. Hu, L. Zhang, *Phys. Rev. B* **2010**, *81*, 1741031 – 1741035; b) S. Cao, T. D. Bennett, D. A. Keen, A. L. Goodwin, A. K. Cheetham, *Chem. Commun.* **2012**, *48*, 7805 – 7807; c) M. Zhou, K. Wang, Z. Men, C. Sun, Z. Li, B. Liu, G. Zou, B. Zou, *CrystEngComm* **2014**, *16*, 4084.
[12] a) K. Suzuki, *J. Non-Cryst. Solids* **1989**, *112*, 23 – 32; b) H. J. Fecht, G. Han, Z. Fu, W. L. Johnson, *J. Appl. Phys.* **1990**, *67*, 1744 – 1748; c) J. Font, J. Muntasell, E. Cesari, *Mater. Res. Bull.* **1997**, *32*, 1691 – 1696; d) M. Nagahama, H. Suga, O. Andersson, *Thermochim. Acta* **2000**, *363*, 165 – 174; e) J. F. Willart, A. De Gusseme, S. Hemon, G. Odou, F. Danede, M. Descamps, *Solid State Commun.* **2001**, *119*, 501 – 505; f) L. C. Zhang, J. Xu, *Mater. Lett.* **2002**, *56*, 615 – 619; g) J. F. Willart, L. Carpentier, F. Danede, M. Descamps, *J. Pharm. Sci.* **2012**, *101*, 1570 – 1577.
[13] H. J. Fecht, E. Hellstern, Z. Fu, W. L. Johnson, *Metall. Trans. A* **1990**, *21*, 2333 – 2337.
[14] a) E. A. R. Duek, C. A. C. Zavaglia, W. D. Belangero, *Polymer* **1999**, *40*, 6465 – 6473; b) L.-M. Wang, G. Li, Z. J. Zhan, L. L. Sun, W. K. Wang, *Philos. Mag. Lett.* **2001**, *81*, 419 – 423.
[15] a) S. J. Billinge, M. G. Kanatzidis, *Chem. Commun.* **2004**, 749 – 760; b) R. B. Neder, V. I. Korsunskiy, *J. Phys. Condens. Matter* **2005**, *17*, S125 – S134; c) P. K. Allan, K. W. Chapman, P. J. Chupas, J. A. Hriljac, C. L. Renouf, T. C. A. Lucas, R. E. Morris, *Chem. Sci.* **2012**, *3*, 2559.
[16] G. N. Greaves, S. Sen, *Adv. Phys.* **2007**, *56*, 1 – 166.
[17] a) M. F. Summers, *Coord. Chem. Rev.* **1988**, *86*, 43 – 134; b) A. V. Kuttatheyil, M. Handke, J. Bergmann, D. Lassig, J. Lincke, J. Haase, M. Bertmer, H. Krautscheid, *Chem. Eur. J.* **2015**, *21*, 1118 – 1124.
[18] S. Hayashi, K. Hayamizu, *Bull. Chem. Soc. Jpn.* **1989**, *62*, 3061 – 3068.
[19] A. B. Cairns, A. L. Goodwin, *Chem. Soc. Rev.* **2013**, *42*, 4881 – 4893.
[20] a) T. Minami, *J. Non-Cryst. Solids* **1985**, *73*, 273 – 284; b) K. R. Seddon, *J. Chem. Technol. Biotechnol.* **1997**, *68*, 351 – 356; c) A. Hayashi, K. Noi, A. Sakuda, M. Tatsumisago, *Nat. Commun.* **2012**, *3*, 856.
[21] K. D. Kreuer, S. Adams, W. Munch, A. Fuchs, U. Klock, J. Maier, *Solid State Ionics* **2001**, *145*, 295 – 306.
[22] a) N. B. Desai, K. Byrappa, G. S. Gopalakrishna, S. Srikantaswamy, A. B. Kulkarni, *Bull. Mater. Sci.* **1987**, *9*, 317 – 321; b) P. Colomban, A. Novak, *J. Mol. Struct.* **1988**, *177*, 277 – 308; c) M. G. Bellino, D. G. Lamas, N. Walsöe de Reca, *Adv. Funct. Mater.* **2006**, *16*, 107 – 113; d) M. Schuster, K. D. Kreuer, H. Steininger, J. Maier, *Solid State Ionics* **2008**, *179*, 523 – 528.
[23] J.-M. Le Meins, O. Bohnke, G. Courbion, *Solid State Ionics* **1998**, *111*, 67 – 75.
[24] A. Zheng, S. J. Huang, S. B. Liu, F. Deng, *Phys. Chem. Chem. Phys.* **2011**, *13*, 14889 – 14901.
[25] a) D. Braga, S. L. Giaffreda, F. Grepioni, A. Pettersen, L. Maini, M. Curzi, M. Polito, *Dalton Trans.* **2006**, 1249 – 1263; b) A. L. Garay, A. Pichon, S. L. James, *Chem. Soc. Rev.* **2007**, *36*, 846 – 855; c) P. J. Beldon, L. Fabian, R. S. Stein, A. Thirumurugan, A. K. Cheetham, T. Friščić, *Angew. Chem. Int. Ed.* **2010**, *49*, 9640 – 9643; *Angew. Chem.* **2010**, *122*, 9834 – 9837.

Received: January 6, 2016
Revised: February 2, 2016
Published online: March 16, 2016

